Macromolecules

Article

pubs.acs.org/Macromolecules

Thermoresponsive Oligo(ethylene glycol) Functionalized Poly-L-cysteine

Xiaohui Fu, Yong Shen, Wenxin Fu, and Zhibo Li*

Beijing National Laboratory for Molecular Sciences (BNLMS), Laboratory of Polymer Physics and Chemistry, Institute of Chemistry, Chinese Academy of Sciences, Beijing 100190, China

Supporting Information

ABSTRACT: A series of new functional amino acids were prepared in high yield via thiol−ene Michael addition between L-cysteine and monomethoxy oligo(ethylene glycol) (OEG) functionalized methacrylates (OEG_xMA) and acrylate (OEG_xA). These OEGylated cysteine derivatives were converted into polymerizable *N*-carboxyanhydride (NCA) monomers using triphosgene. Subsequent ring-opening polymerization (ROP) of these NCA monomers gave a series of OEGylated poly-L-cysteine (poly-EG_xMA-C or poly-EG_xA-C) homopolypeptides. Depending on the length of OEG side chains, poly-EG_xMA-C and poly-EG_xA-C polypeptides displayed different solubility and secondary structure in water. More importantly, the obtained polypeptides can display reversible thermoresponsive properties in water when the *x* value is between 3 and 5. The synthetic strategy represents a highly efficient method to prepare nonionic functional polypeptides with tunable thermoresponsive properties.

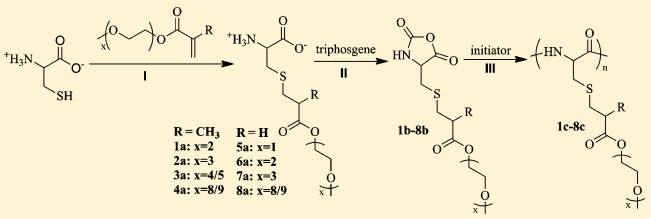

INTRODUCTION

Thermoresponsive polymers can undergo a reversible phase transition from solvated status to insoluble status upon temperature change.[1] Given such a unique temperature induced stimuli-responsive feature, thermoresponsive polymers are extensively explored in applications of bio- and nanotechnology.[2,3] For example, they can be used to construct smart drug delivery system, thermoresponsive hydrogels, smart surface, etc.[4] In contrast to conventional thermoresponsive polymers, biodegradable counterparts are of critical importance for biomedical applications given their advantages in biocompatibility and biodegradability.[5−8] Toward this goal, several biodegradable thermoresponsive polymer systems were reported, such as polyesters,[9,10] poly(amino ester)s,[11] poly(organophosphazenes),[12] and poly(amino acids).[13−17] Among them, the polypeptide materials attract great research interests because they can not only be modified with different functional groups but also offer additional higher ordering from their inherent secondary structures, e.g., α-helix vs β-sheet, which can be modulated via external stimuli.[7,8] In this regard, synthetic stimuli-responsive polypeptide materials are under intensive research in recent years.

In addition to solid phase synthesis, polypeptide materials can be prepared via ring-opening polymerization of *N*-carboxyanhydride (NCA) monomers.[18−20] Great progresses were recently made to prepare stimuli-responsive polypeptide materials.[7,8] For example, Kramer and Deming reported preparation of sugar functionalized cysteine, from which they constructed redox responsive glycopolypeptides.[21,22] Most recently, they demonstrated a general route to make multifunctional and multiactive polypeptides by postalkylation of polymethionine.[23] Zhang et al. reported a general strategy to make side chain functionalized helical polypeptides containing halide or azide groups.[24] Combining ATRP and ROP, Chen and co-workers prepared thermoresponsive polypeptides based on polyglutamate derivatives.[17] Schlaad and co-workers prepared pH-responsive and bioactive glycopolypeptides using ROP and postmodifications.[25] Most recently, they reported preparation of thermoresponsive poly(N-C3 glycine)s.[16] Photoresponisve polypeptides were also prepared via ROP of functional cysteine NCA.[26] On the other hand, thermoresponsive polypepides were prepared from di- and triethylene glycol functionalized poly-L-glutamate (poly-L-EG_xGlu).[13,14] We demonstrated that their thermoresponsive propertiesdepended not only on the side chain length but also on the chirality of polypeptide backbone.[15] The formation of stable helical conformation is necessary for the well-defined low critical solution temperature (LCST) behaviors.[15]

It was well-known that oligo(ethylene glycol) (OEG) functionalized monomers can be used to prepare thermoresponsive polymers,[27,28] and LCST of obtained polymers can be tuned through variation of side chain length or copolymerization of different monomers.[29,30] The most well-known examples were the OEGylated methacrylates and acrylates. Additionally, conjugation of OEG onto benzyl ring of styrene can also generate thermoresponsive polymers.[27,31] It is generally accepted that the thermoresponsive properties arise from the reversible dehydration and rehydration of OEG

Received: April 2, 2013
Revised: April 21, 2013
Published: April 30, 2013

Scheme 1. Synthetic Routes toward Poly-EG$_x$MA-C (1c−4c) and Poly-EG$_x$A-C (5c−8c) Homopolypeptides[a]

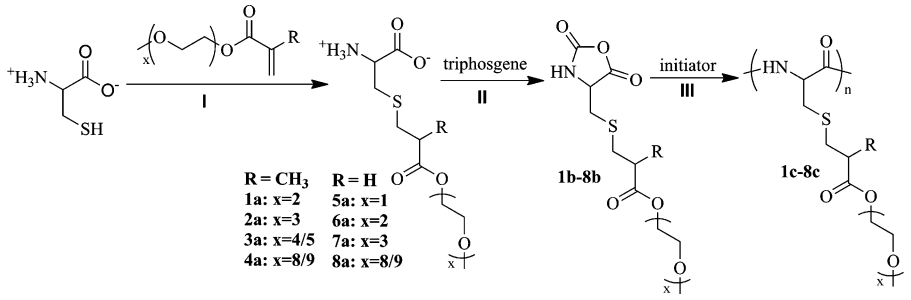

[a]Reagents and conditions: (I) OEG$_x$MA or OEG$_x$A, H_2O, pH = 7.5, 88−96% yield; (II) triphosgene, THF, 50 °C, 65−80% yield; (III) Et_3N, THF, 30 °C, 60−80% yield.

moieties upon temperature change. However, conjugation of OEG moieties onto polypeptide side chain usually does not endow thermoresponsive properties to polypeptides. For example, OEGylated poly-L-lysine formed stable helical structure in water and did not have thermoresponsive properties.[32] In contrast, OEGlyated poly-L-serine formed β-sheet structure in water and also did not show thermoresponsive properties, whereas only OEGlyated poly-L-glutamates displayed thermoresponsive properties.[13−15] The reason is probably that the solution properties of OEGylated polypeptides not only depended on substructure of side chains but also relied on their inherent secondary structures.

Hence, it is of particular interest and importance to develop novel and highly efficient methods to make thermoresponsive polypeptides from easily available chemicals. Herein, we report an unprecedented way to make a series of OEGylated α-amino acids using thiol−ene Michael addition between cysteine and oligo(ethylene glycol) (meth)acrylates (OEG$_x$MA or OEG$_x$A) with high efficiency and high yield. Importantly, most OEG$_x$(M)A monomers are commercially available or easy to make from available monomers. More interestingly, some of these OEGylated poly-L-cysteine homopolypeptides show thermoresponsive properties in water and their LCSTs varied with side chain length.

EXPERIMENTAL SECTION

Materials and Instruments. Hexane, tetrahydrofuran (THF), and dichloromethane (DCM) were purified by first purging with dry nitrogen, followed by passing through columns of activated alumina. *N*,*N*-Dimethylformamide (DMF) was treated with free amine scavenger (Aldrich) before passing through 4 Å molecular sieves and activated alumina column. Et_3N was refluxed with sodium and freshly distilled before use. Deionized water (18 MΩ·cm) was obtained from a Millipore Milli-Q purification unit. All commercial reagents were used as received without further purification unless otherwise stated. ^{1}H NMR spectra and ^{13}C NMR spectra were recorded on Bruker AV400 FT-NMR spectrometer. Electrospray ionization tandem mass spectrometry (ESI-MS) was recorded on a Shimadzu Inc. LCMS-2010 spectrometer. All infrared spectroscopy measurements were performed using a Nicolet Avatar 330 FT-IR spectrometer. The solution samples were cast on KBr plates before measurement. The solid samples was milled with potassium bromide (Aldrich) at mass ratio of 1:100 and pressed into disk before IR measurements. Tandem size exclusion chromatography/laser light scattering (SEC/LLS) was performed at 50 °C using an SSI pump connected to Wyatt Optilab DSP and Wyatt DAWN EOS light scattering detectors with 0.02 M LiBr in DMF as eluent at flow rate of 1.0 mL/min. All SEC/LLS samples were prepared at concentrations of about 5 mg/mL. The clouding points (CPs) were measured by monitoring the transmittance of a 500 nm light beam through a quartz sample cell at concentration of 2 mg/mL on a Shimadzu UV−vis spectrometer. The solution was heated or cooled at rate of 0.5 °C/min. The CP was defined as the temperature corresponding to 50% transmittance of aqueous solution during the heating process. Circular dichroism spectra were recorded on an Applied Photophysics Chirascan CD spectrometer. The solution was placed into a quartz cell with a path length of 1.0 mm, and the concentration of samples was 0.5 mg/mL. For the temperature-dependent experiments, the temperature of the sample chamber, where the quartz cell was placed, was controlled by a water bath. The secondary structures was analyzed on DICHROWEB using Contin-LL.[33,34]

Synthesis of 2-(2-Methoxyethoxy)ethoxyethyl Methacrylate (EG$_3$MA). Solution of methacryloyl chloride (13.0 g, 124.8 mmol) in dry DCM (20 mL) was added dropwisely into a mixture of tri(ethylene glycol) monomethyl ether (20.5 g, 124.8 mmol), triethylamine (12.6 g, 124.8 mmol), DMPA (0.76 g, 6.24 mmol), and DCM (60 mL) under vigorous stirring at 0 °C. The reaction mixture was stirred at 0 °C for about 2 h and overnight at room temperature. After that, the mixture was filtered to remove triethylamine hydrochloride salt. The filtrate was then washed sequentially with 25 mL of 1 N HCl solution twice, saturated $NaHCO_3$ aqueous solution, and brine solution. The organic phase was dried using anhydrous $MgSO_4$, and the solvent was removed under reduced pressure to give the product as light yellow oil (21.5 g, 74% yield). ^{1}H NMR (400 MHz, $CDCl_3$): δ (ppm) 6.10 (s, 1H), 5.54 (s, 1H), 4.26 (t, 2H), 3.71 (t, 2H), 3.63 (t, 6H), 3.52 (t, 2H), 3.34 (s, 3H), 1.92 (s, 3H). Using the same procedure, we prepared another three monomers, i.e., 2-methoxyethyl acrylate (EG$_1$A), 2-methoxyethoxy ethyl acrylate (EG$_2$A), and 2-(2-methoxyethoxy)ethoxy ethyl acrylate (EG$_3$A). The corresponding characterizations can be found in the Supporting Information.

General Procedure for Synthesis of OEGylated Cysteine Derivatives [EG$_x$(M)A-C] (1a−8a). L-Cysteine (5.0 g, 31.7 mmol) was dispersed in 50 mL water, and the solution pH was then tuned to 7.5 using 1 N NaOH solution. Next, 1.1 mol equiv EG$_3$MA monomer was added to the mixture. Then the solution was stirred overnight at room temperature, and subsequently washed using 50 mL ethyl acetate three times to remove unreacted EG$_3$MA. After that, the aqueous phase was lyophilized to give the product as a pale yellow solid with 95% yield. Using the same procedure, we prepared 8 OEGylated L-cysteine and 8 D-cysteine derivatives as illustrated in Scheme 1. The corresponding molecular characterizations of these monomers can be found in the Supporting Information.

General Procedure for Synthesis of OEGylated L-Cysteine NCA [EG$_x$MA-C or EG$_x$A-C NCAs] (1b−8b). A typical example is described below. To a mixture of EG$_x$MA-C and triphosgene (0.39 equiv), anhydrous THF was added. The mixture was then heated to 50 °C for 5 h, and the solution turned to clear within 3 h. Solvent was then removed under reduced pressure to give yellow oil. The crude product was fractionally precipitated from THF using hexane to yield pale yellow oil with 78% yield. Using the same procedure, we prepared 16 NCA monomers, and the corresponding characterizations are shown in the Supporting Information.

General Procedure for ROP of EG_xMA-C or EG_xA-C NCAs. The ROP of EG_xMA-C NCA was performed in THF using Et_3N as initiator under N_2 purge. Typically, Et_3N/THF (20 mg/mL) solution was injected into NCA/THF solution (50−100 mg/mL), and the solution was then stirred at 30 °C for 48 h. The product was precipitated using excess hexane and characterized using SEC/LLS. The collected product was dissolved in H_2O and transferred to dialysis tubing (COMW = 3500 Da). The sample was dialyzed against deionized water for 3 days with water changed per 12 h. Dialyzed polymers were lyophilized to yield poly-EG_xMA-C and poly-EG_xA-C homopolypeptides (**1c**−**8c**) as white solids. The yield was between 65% and 80% for different samples. Using the same procedure, we prepared 16 OEGylated polycysteine homopolypeptides, i.e., **1c**−**8c** and $\mathbf{1c^D}$−$\mathbf{8c^D}$, respectively. The corresponding molecular characterizations are given in the Supporting Information.

RESULTS AND DISCUSSION

For the comprehensive investigation of OEG side chain length on physical properties of these OEGylated polycysteine, we synthesized **2a**, **5a**−**7a** four new monomers in addition to commercially available OEGMA and OEGA monomers (Scheme 1). The monomers were prepared by direct coupling between (meth)acryl chloride and commercially available monomethoxy oligo(ethylene glycol). The chemical structures of **2a** and **5a**−**7a** were confirmed by ^{1}H NMR spectrometry (see Supporting Information). Figure 1a shows the ^{1}H NMR spectrum of OEG_3MA monomer, which shows characteristic resonances of methacrylate and OEG moieties. The resonances at 1.9, 5.5, and 6.1 ppm are attributed to protons of methyl and methylene groups in methacrylate. Resonance at 4.3 ppm is methylene protons next to ester bond. Resonance at 3.4 ppm is protons of methoxy group. The resonances from 3.5 to 3.7 ppm are methylene groups of ethylene glycol units. The samples of **3a**/**b**/**c**, **4a**/**b**/**c**, and **8a**/**b**/**c** were derived from commercial OEGMA and OEGA monomers with formulate weight being 300, 475, and 480 g/mol, respectively. For these three series of samples, the monomers were actually a mixture of at least two species, and the average repeating unit of OEG side chains was between 4 and 5 or 8 and 9, respectively.

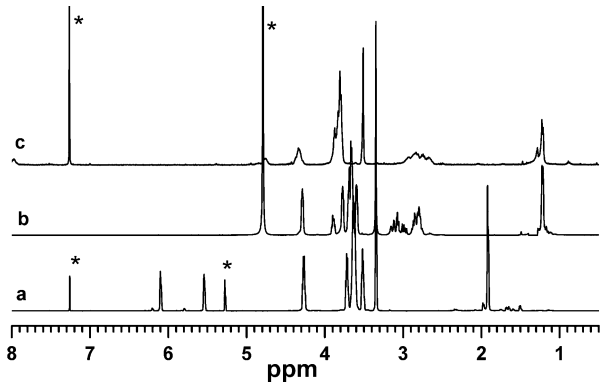

Figure 1. ^{1}H NMR spectra of (a) OEG_3MA monomer in $CDCl_3$, (b) **2a** (L-EG_3MA-C) in D_2O, and (c) **2c** (poly-L-EG_3MA-C) in $CDCl_3$.

Thiol−ene Michael addition shares many characteristics of click reaction.[35,36] The reaction is highly efficient under benign condition and has high tolerance of functional groups. Besides, there are no byproducts to complicate the product purification. As illustrated in Scheme 1, the thiol group in cysteine can directly react with the double bond of (meth)acrylate monomers (**1a**−**8a**) in weak basic condition (pH = 7.5−8) at room temperature. The reaction was fast and quantitative with yield above 95%. Figure 1b gives the ^{1}H NMR spectrum of **2a** (L-EG_3MA-C). The peaks of methacrylate group at 5.5 and 6.1 ppm completely disappear, which indicates the quantitative conversion of OEG_3MA. In addition, the appearance of new peaks at 1.3 ppm and broad peaks between 2.7 and 3.3 ppm, which corresponds to the methine and methylene, respectively, indicates successful addition between cysteine and OEG_3MA. Note that it is necessary to keep the solution pH weak basic in order to enhance the reactivity of mercapto group. On the other hand, insoluble byproducts were observed when pH was over 8. Moreover, the amine group can undergo aza-Michael addition with acrylates to produce byproducts under basic conditions. Although the deprotonated amine groups do not react with OEG_xMA monomers without catalyst, they can attack the ester bonds via amidation. We found that when pH was between 7.5 and 8, the thiol−ene addition had great selectivity and efficiency to give clean products, which can be purified via simple wash to give solid products.

Subsequently, monomers **1a**−**8a** were converted to corresponding NCAs (**1b**−**8b**) using triphosgene in THF at 50 °C under N_2 purge. The obtained NCAs were generally viscous oil at room temperature, which were then fractionally precipitated from THF using hexane (THF/hexane = 1:3) to yield the product as pale yellow oil. All NCA monomers (**1b**−**8b**) are readily soluble in common solvents such as THF, ethyl acetate, DCM, and DMF, except hexane and ethyl ether. To study the effects of chirality, we also used D-cysteine to react with all OEG_xMA and OEG_xA monomers. The corresponding products are designated as $\mathbf{1a^D}$−$\mathbf{8a^D}$. The superscript D represents D-cysteine monomer. The default monomer is L-cysteine in the remaining text except where noted. Their structures are unambiguously characterized as shown in the Supporting Information.

For the obtained OEG functionalized cysteine NCA monomers (**1b**−**8b**), a big challenge is the NCA purification. Beside THF/hexane mixture, we also tried using different solvent pairs, but it did not solve the problem to offer high purity NCAs. The reason we believe is due to the OEG units, especially for samples **4b** and **8b**, which have the longest OEG side chain among studied monomers. These NCA monomers are viscous oil after fractional precipitation. After at least three times fractional precipitation, these NCAs can be polymerized using Ni(0) complex, primary amine, and hexmethyldisilane (HMDS) as initiators, whereas the efficiency was generally low. We also tried to use flash column chromatography to purify NCA however without success.[23] For example, samples **4b** and **8b** underwent self-polymerization during the flash column chromatograph process.

Due to the difficulty of NCA purifications, we then used Et_3N as initiator to perform ROP in THF at 30 °C except **1b** because its polymer (**1c**) precipitated in THF during polymerization. After polymerization, the obtained homopolypeptides were precipitated using hexane and subsequently purified via dialysis against deionized water. The products were obtained as white solid after lyophilization. The molecular weight and molecular weight distribution were characterized using SEC/LLS, and the corresponding results of **1c**−**8c** and $\mathbf{1c^D}$−$\mathbf{8c^D}$ are summarized in Table S1. Figure 1c shows the ^{1}H NMR spectrum of **2c**, which agrees well with expected structure. Table S1 summarizes the molecular parameters of 16 samples. Although we used tertiary amine as initiator, the molecular weight distributions of obtained samples were relatively narrow. The main reason was that the molecular

dx.doi.org/10.1021/ma400678w | Macromolecules 2013, 46, 3753−3760

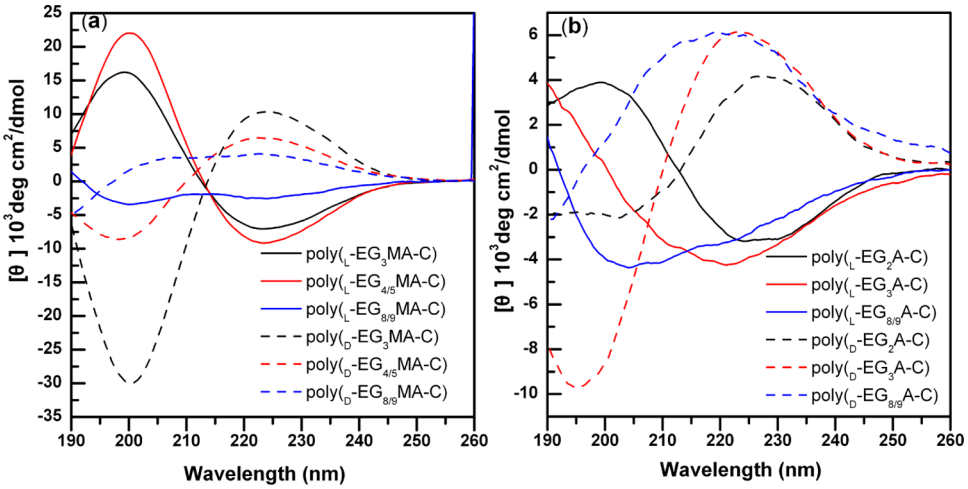

Figure 2. CD spectra of different OEGylated polycysteine homopolypeptides: (a) poly-L-EG$_x$MA-C (solid line) and poly-D-EG$_x$MA-C (dashed line); (b) poly-L-EG$_x$A-C (solid line) and poly-D-EG$_x$A-C (dashed line).

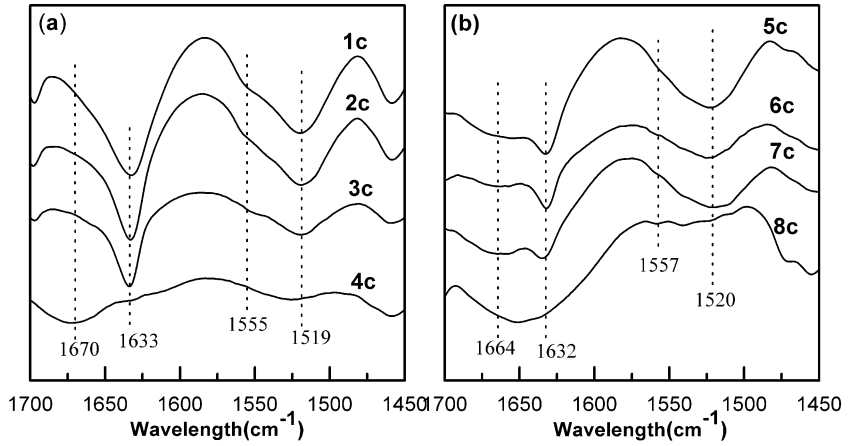

Figure 3. FTIR spectra of (a) poly-L-EG$_x$MA-C and (b) poly-L-EG$_x$A-C homopolypeptides in solid state. The captions of **1c**−**8c** are the same as Scheme 1.

weights of most samples were relatively low. Next, we will focus on the solution properties of obtained homopolypeptides, i.e., **1c**−**8c** and **1c**^{D}−**8c**^{D}.

We first examined the aqueous solution properties of **1c**−**8c**, and the corresponding solubility data are summarized in Table S2. It was found that their solubility in water increased with the OEG side chain length. All samples had good solubility in common organic solvents except **5c**, which became insoluble in most organic solvents after precipitation from DMF. The reason was that **5c** formed stable β-sheets, which was similar to poly-L-EG$_1$Glu homopolypeptide.[14] The results were also supported by FTIR measurements shown in Figure 3. Increasing side chain length from one OEG unit to two slightly increased samples' solubility in water. For example, sample **6c** was partially soluble in water. When the repeat number of OEG units was larger than 2, samples of **2c**−**4c** and **7c**−**8c** were readily soluble in water at room temperature and buffer solutions.

It was known that the secondary structures of proteins facilitate the folding of proteins into unique three-dimensional structures and regulated their biological activities.[37] The secondary structure of polypeptides can be affected not only by the chain length but also by the steric and chemical compatibility of side chains.[38] Considering this, we investigated the effects of OEG side chain length on the secondary structures of poly-L-cysteine derivatives using circular dichroism (CD) and FTIR spectroscopy. It was known that poly-L-cysteine was β-sheet forming polypeptide.[39] Previous studies showed that conjugation of di(ethylene glycol) thioester to the poly-L-cysteine side chain did not disrupt polymer's β-sheet conformation.[40] In contrast, poly-L-cysteine conjugated with hydrophilic sugars adopted helical conformation.[21] Figure 2 compares the CD spectra of **2c**−**4c** and **6c**−**8c** homopolypeptides in water, respectively. Apparently, CD characterizations revealed that both series of samples formed mixed conformation, in which random coil was the major conformation. These were different from the conformation of OEGylated poly-L-glutamates[41] and OEGlyated poly-L-lysine.[32] For samples derived from OEG$_x$MA monomers, the α-helical content was about 7%, while the β-strand content changed from 43% to 45.5% and to 27% when the OEG repeat units increased from 3 to 4/5 and to 8/9 (Table S3). In contrast, the α-helical content increased slightly with OEG chain length for homopolypeptides derived from OEG$_x$A monomers. For example, the helical contents were about 6%, 8%, and 12% for sample **6c**, **7c**, and **8c**, respectively. Meanwhile, the corresponding β-strand content decreased from 36% to 24% (Table S3). There were two possible reasons for these poly-L-cysteine derivatives to

dx.doi.org/10.1021/ma400678w | *Macromolecules* 2013, 46, 3753−3760

form mixed secondary conformation. One was that the long side chain could destabilize the stability of secondary structure. The synthetic method of poly-L-EG$_x$MA-C or poly-L-EG$_x$A-C homopolypeptides made them have longer side chains than poly-L-EG$_x$Glu. This is also consistent with polypeptide brushes, in which the elongation of side chain decreased the helicity of polypeptide backbones.[42−44] The other possible reason was that the molecular weights were not high enough, which might seriously affect the content of secondary conformation. Compared to poly-L-EG$_x$A-C counterparts, poly-L-EG$_x$MA-C samples had one more methyl group, which accordingly disrupted the regularity of side chains. This might be the reason that accounted for relative high helicity for poly-L-EG$_x$A-C samples than poly-L-EG$_x$MA-C counterparts. Figure 2 also presents the CD spectra of corresponding homopolypeptides prepared from D-cysteine. They displayed similar secondary structure to their counterparts, i.e., poly-L-EG$_x$MA-C and poly-L-EG$_x$A-C.

Furthermore, the conformation of both series of samples at solid state was characterized using FTIR shown in Figure 3. For samples **1c**−**4c**, FTIR spectra shown in Figure 3a indicate that these four samples mainly adopted β-sheet conformation. All four samples displayed strong absorbance at 1635−1631 cm^{-1} (amide I) and 1523−1517 cm^{-1} (amide II), which were characteristics of β-sheet structures.[45] From sample **1c** to **4c**, the increase of absorbance at 1650−1670 cm^{-1} and the decrease of absorbance at 1620−1630 cm^{-1} indicated relative increase of helicity for sample **1c** to sample **4c**. These results suggested that helical conformation increased with OEG side chain length, which was consistent with that of poly-L-EG$_x$Glu samples.[14,15] This trend is interestingly opposite to CD results. The reason was probably that the CD spectra were recorded in solution, in which the steric effects of solvated OEG side chains may predominate. The FTIR measurements were done in dried status. It is worth noting that the sample **5c** (poly-L-EG$_1$A-C), which was insoluble in water and most organic solvents, displays strong absorption bands at 1632 cm^{-1} (amide I band) and 1520 cm^{-1} (amide II band), indicating predominate β-strand conformation (Figure 3b).

We then investigated the effects of temperature on samples' solubility in water and found that samples **2c**, **3c**, and **7c** displayed reversible thermoresponsive properties in water. Figure 4 shows the transmittance versus temperature plots for dilute solution of **2c**, **3c**, and **7c**. Sample **2c** with DP = 26 showed a clear LCST type phase transition with increase of temperature, and the CP was about 50 °C. Generally, increasing OEG side chain length will increase polymer's solubility in water as well as the corresponding CP.[3,46] Compared to sample **2c**, sample **3c** containing one more OEG units showed a sharper phase transition with CP = 65 °C (Figure 4). Furthermore, sample **4c** was completely soluble in water without showing observable thermoresponsive behaviors until water boiling. On the other hand, the substructure of precursor was also important toward polymers' properties. Sample **5c** was insoluble in water, and sample **6c** was only partially soluble in water. Sample **7c** had a less methyl group than sample **2c**, so it presumably should have better solubility than **2c**. Under similar conditions, sample **7c** had a CP = 51 °C, which was 1 deg higher than that of sample **2c**. In particular, the CP determined from cooling ramp was about 8, 4, and 10 °C lower than heating ramp for samples **2c**, **3c**, and **7c**, respectively. We presumed the hysteresis of CP between heating and cooling cycle was due to the intermolecular hydrogen bonding, which

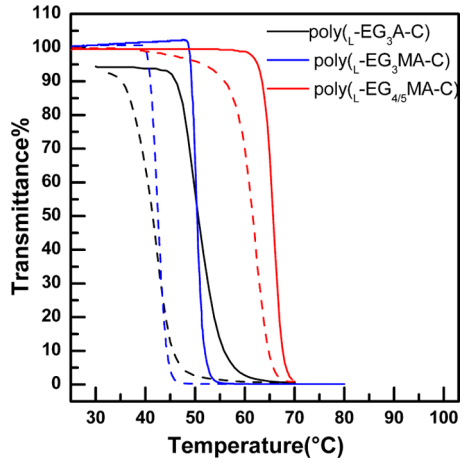

Figure 4. Plots of transmittance as a function of temperature for aqueous solutions (2 mg/mL) of **2c** (poly-L-EG$_3$MA-C), **3c** (poly-L-EG$_{4/5}$MA-C), and **7c** (poly-L-EG$_3$A-C). Solid line: heating; dashed line: cooling.

required slight overcooling to overcome the energy barrier.[47] It was well-known that a delicate hydrophilic/hydrophobic balance was necessary to achieve thermoresponsive properties for polymers. For poly-L-EG$_x$A-C and poly-L-EG$_x$MA-C homopolypeptides, there are two functional groups that can interact with water to form hydrogen bonding. One is the OEG side chains; the other is amide bonds within the backbone. Elongation of OEG length will increase polymer hydrophilicity and accordingly will increase the phase transition temperature until losing thermoresponsive properties, e.g., **4c** and **8c**. On the opposite, if the OEG side chains were too short, their hydrophilic contributions were not enough to compensate for the overall hydrophobicity of other units. As a result, the polymers were not soluble in water, e.g., **1c** and **5c**. For OEGylated polycysteine derivatives, we demonstrated that only when the repeat units of OEG were between 3 and 5, the obtained polycysteine derivatives reached a hydrophilic and hydrophobic balance to obtain thermoresponsive properties. The exact phase transition temperature varied with OEG length. On the other hand, the amide bonds of backbone can also affect the hydrophilicity of samples. If the polypeptides adopted random coil conformation, amide bonds preferred forming hydrogen bonding with water, which will increase samples' hydrophilicity as expected. If the polypeptides adopted α-helical conformation, the amide bonds predominately formed intramolecular hydrogen bonding, which made them less hydrophilic than the random coil counterparts. Note that OEGylated polycysteine derivatives need more ethylene glycol units to obtain thermoresponsive properties as compared to OEGylated polyglutamate.[14,15] The reason we believed was due to the additional ethylene groups from (me)acrylate. Because of the multiple hydrogen bonding interactions, polypeptide had more complicated thermoresponsive mechanism than poly(*N*-isopropylacrylamide).

To study the effects of temperature on polypeptide's conformation, we carried out temperature varied CD measurements for samples of **2c**, **3c**, and **7c**. Figure 5 shows the corresponding CD spectra at different temperature in heating ramp. Apparently, all three samples did not show substantial conformation changes upon temperature increase within experimental time range. For sample **2c**, β-sheet content slightly increased with increase of temperature (Figure 5a). For

dx.doi.org/10.1021/ma400678w | *Macromolecules* 2013, 46, 3753−3760

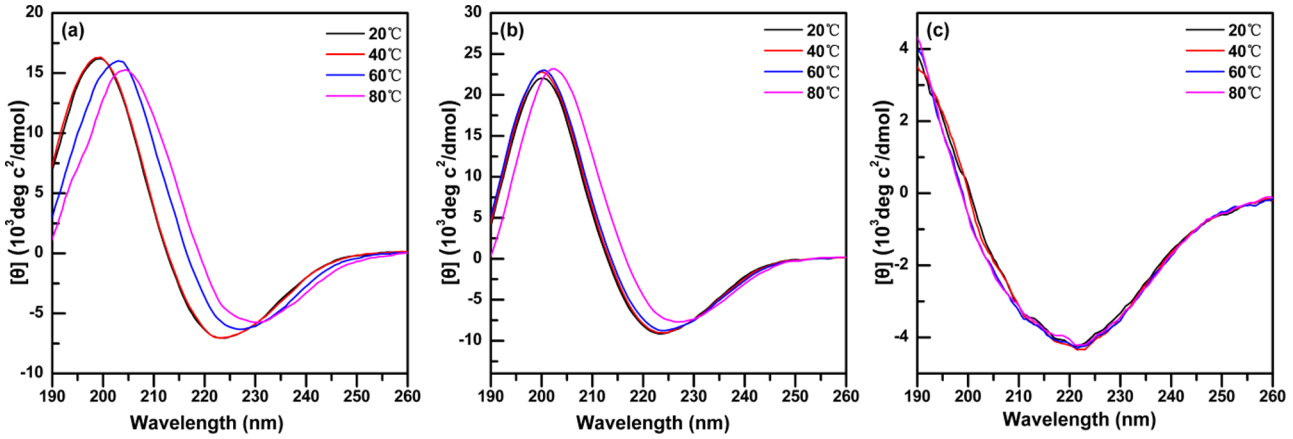

Figure 5. Secondary structure dependence on temperature for OEGylated polycysteine derivatives: (a) sample **2c** (poly-L-EG_3MA-C), DP = 26; (b) sample **3c** (poly-L-$EG_{4/5}$MA-C), DP = 54; (c) sample **7c** (poly-L-EG_3A-C), DP = 47. The concentration is 0.5 mg/mL.

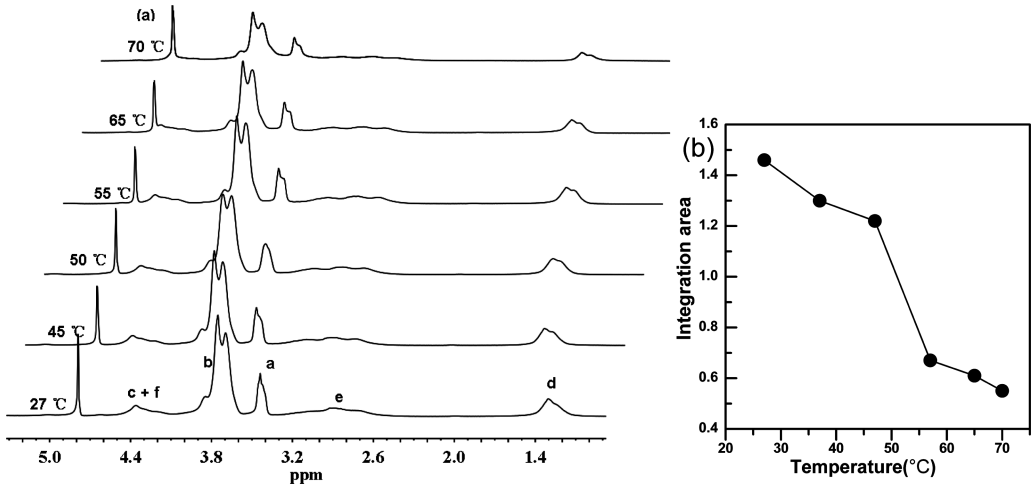

Figure 6. (a) Temperature varied ^{1}H NMR for sample **3c** (poly-L-$EG_{4/5}$MA-C) with DP = 54 and concentration = 3 mg/mL in D_2O and (b) plot of the integration area of $-OCH_3$ versus temperature.

sample **3c**, the β-sheet content increased when the solution was heated above its CP (Figure 5b). Whereas, there was little change observed for sample **7c** during the heating process (Figure 5c). For all three samples, their conformation dependence on temperature was reversible, which was consistent with turbidity measurements shown in Figure 4. For all three samples, their CD spectra in cooling ramp were similar to their heating ramp as shown in the Supporting Information.

We have demonstrated that samples **2c**, **3c**, and **7c** displayed reversible LCST behaviors in water. It was important to understand the underlying mechanism regarding the driving force for the thermoresponsive properties. We thus applied temperature-dependent ^{1}H NMR to explore the local chemical environmental variation of these characteristic protons, e.g., methylene and methoxy in OEG groups, versus temperature (Figure 6). At room temperature, the protons of methoxy group ($\delta \sim 3.4$) and methylene ($\delta \sim 3.6$) of OEG units were easily identified for samples of **2c**, **3c**, and **7c** (Figures S11 and S12). With increase of temperature, we found that resonance peaks of end methoxy and methylene groups became broader, accompanying a substantial decrease in signal intensity. Further increasing temperature above their CPs caused almost disappearance of their resonances. These results suggested that increasing temperature induced dehydration of OEG groups, which caused the aggregation of polypeptides. Also, the CD results shown in Figure 5 indicated that heating do not disrupt samples' preformed conformation. The integration areas of protons belonging to OEG side chain can be used as a semiquantitative method to evaluate the temperature-induced transition. Figure 6b presents plot of normalized integration area of methoxy group versus temperature, which displays a similar transition to turbidity experiment. Taking the middle point of transition temperature, we can estimate the CP being about 60 °C, in good agreement with turbidity measurements. Above all, temperature varied ^{1}H NMR measurements suggested that the thermoresponsive behaviors mainly arose from the thermoresponsive of OEG side chains.

Moreover, we also explored effects of polypeptide chirality toward their LCST behaviors. Using D-cysteine, we synthesized poly-D-EG_xMA-C (**1c^D**−**4c^D**) and poly-D-EG_xA-C (**5c^D**−**8c^D**). Overall, these OEGylated poly-D-cysteine homopolypeptides had similar properties in terms of solubility and conformation as compared to samples **1c**−**8c**. For example, samples **2c^D**, **3c^D**, and **7c^D** displayed CP around 66, 65, and 68 °C, respectively (Figure S1). Similar to sample **3c**, sample **3c^D** with DP = 24 displayed reversible LCST behaviors in water with CP = 65 °C (Figure S1a). Note that sample **7c^D** has higher CP than **7c**. We

dx.doi.org/10.1021/ma400678w | *Macromolecules* 2013, 46, 3753−3760

attributed this difference to the optical purity arising from synthetic D-cysteine.

The effects of sample concentration on the phase transition temperature of **2c**, **3c**, and **7c** were examined. As shown in Figure S13, the LCST was found to decrease progressively with concentration between 0.5 and 2 mg/mL, but the decrease became negligible when the concentration was above 2 mg/mL. The reason we assumed was due to the intermolecular aggregation behaviors, which was enhanced with concentration increase.[48] In this study, the influence of salt concentration on the LCST was also studied. A typical "salting-out" effect was observed in our tests (Figure S14). As the salt concentration increased, the CPs of sample **2c**, **3c**, and **7c** all had obvious decrease. For example, the CPs of sample **2c**, **3c**, and **7c** had 4, 5, and 10 deg decrease, respectively, when the NaCl concentration changed from 0 to 8 mg/mL. The possible reason was that the presence of NaCl results in a partial dehydration of OEG side chains, which caused decrease of samples' hydrophilicity to water.[28]

CONCLUSION

In summary, we demonstrated a facile and economic strategy to prepare biodegradable, nonionic thermoresponsive polypeptides based on cysteine and OEGylated (meth)acrylates. Using easily available starting materials, a series of OEGlyated cysteine derivatives were synthesized using thiol−ene Michael addition, which benefited from mild reaction conditions, minimal byproduct formation, high functional group tolerance, and high yields. Depending on the length of OEG side chain, the obtained OEGlated poly-L-cysteine derivatives had different solution properties but had thermoresponsive behaviors only when the repeat unit of OEG was between 3 and 5. We believed that such biodegradable thermoresponsive polypeptides might be promising candidates to construct new intelligent biomaterials for biomedical applications.

ASSOCIATED CONTENT

Supporting Information

Experimental details and characterization; additional CD, UV−vis, FTIR, and NMR spectra. This material is available free of charge via the Internet at http://pubs.acs.org.

AUTHOR INFORMATION

Corresponding Author

*E-mail: zbli@iccas.ac.cn (Z.L.).

Notes

The authors declare no competing financial interest.

ACKNOWLEDGMENTS

The authors appreciate financial support from the National Natural Science Foundation of China (20974112, 50821062, and 91027043), Chinese Academy of Sciences (XDA01030302).

REFERENCES

(1) Roy, D.; Cambre, J. N.; Sumerlin, B. S. *Prog. Polym. Sci.* **2010**, *35*, 278−301.
(2) Schmaljohann, D. *Adv. Drug Delivery Rev.* **2006**, *58*, 1655−1670.
(3) Lutz, J.-F. *Adv. Mater.* **2011**, *23*, 2237−2243.
(4) Stuart, M. A. C.; Huck, W. T. S.; Genzer, J.; Muller, M.; Ober, C.; Stamm, M.; Sukhorukov, G. B.; Szleifer, I.; Tsukruk, V. V.; Urban, M.; Winnik, F.; Zauscher, S.; Luzinov, I.; Minko, S. *Nat. Mater.* **2010**, *9*, 101−113.
(5) Liu, F.; Urban, M. W. *Prog. Polym. Sci.* **2010**, *35*, 3−23.
(6) Löwik, D. W. P. M.; Leunissen, E. H. P.; van den Heuvel, M.; Hansen, M. B.; van Hest, J. C. M. *Chem. Soc. Rev.* **2010**, *39*, 3394.
(7) He, C.; Zhuang, X.; Tang, Z.; Tian, H.; Chen, X. *Adv. Health Mater.* **2012**, *1*, 48−78.
(8) Zhang, S.; Li, Z. *J. Polym. Sci., Part B: Polym. Phys.* **2013**, *51*, 546−555.
(9) Zhang, L.-J.; Dong, B.-T.; Du, F.-S.; Li, Z.-C. *Macromolecules* **2012**, *45*, 8580−8587.
(10) Ajiro, H.; Takahashi, Y.; Akashi, M. *Macromolecules* **2012**, *45*, 2668−2674.
(11) Wu, D.-C.; Liu, Y.; He, C.-B. *Macromolecules* **2007**, *41*, 18−20.
(12) Lee, S. B.; Song, S.-C.; Jin, J.-I.; Sohn, Y. S. *Macromolecules* **1999**, *32*, 7820−7827.
(13) Liao, Y.; Dong, C.-M. *J. Polym. Sci., Part A: Polym. Chem.* **2012**, *50*, 1834−1843.
(14) Chen, C.; Wang, Z.; Li, Z. *Biomacromolecules* **2011**, *12*, 2859−2863.
(15) Zhang, S.; Chen, C.; Li, Z. *Chin. J. Polym. Sci.* **2013**, *31*, 201−210.
(16) Robinson, J. W.; Secker, C.; Weidner, S.; Schlaad, H. *Macromolecules* **2013**, *46*, 580−587.
(17) Ding, J.; Xiao, C.; Zhao, L.; Cheng, Y.; Ma, L.; Tang, Z.; Zhuang, X.; Chen, X. *J. Polym. Sci., Part A: Polym. Chem.* **2011**, *49*, 2665−2676.
(18) Hadjichristidis, N.; Iatrou, H.; Pitsikalis, M.; Sakellariou, G. *Chem. Rev.* **2009**, *109*, 5528−5578.
(19) Kricheldorf, H. R. *Angew. Chem., Int. Ed.* **2006**, *45*, 5752−5784.
(20) Cheng, J.; Deming, T. J. *Top. Curr. Chem.* **2011**, *310*, 1−26.
(21) Kramer, J. R.; Deming, T. J. *J. Am. Chem. Soc.* **2010**, *132*, 15068−15071.
(22) Kramer, J. R.; Deming, T. J. *J. Am. Chem. Soc.* **2012**, *134*, 4112−4115.
(23) Kramer, J. R.; Deming, T. J. *Biomacromolecules* **2012**, *13*, 1719−1723.
(24) Tang, H.; Zhang, D. *Biomacromolecules* **2010**, *11*, 1585−1592.
(25) Krannig, K.-S.; Schlaad, H. *J. Am. Chem. Soc.* **2012**, *134*, 18542−18545.
(26) Liu, G.; Dong, C.-M. *Biomacromolecules* **2012**, *13*, 1573−1583.
(27) Zhao, B.; Li, D.; Hua, F.; Green, D. R. *Macromolecules* **2005**, *38*, 9509−9517.
(28) Lutz, J.-F.; Akdemir, Ö.; Hoth, A. *J. Am. Chem. Soc.* **2006**, *128*, 13046−13047.
(29) Lutz, J.-F.; Weichenhan, K.; Akdemir, Ö.; Hoth, A. *Macromolecules* **2007**, *40*, 2503−2508.
(30) Lutz, J.-F.; Hoth, A. *Macromolecules* **2006**, *39*, 893−896.
(31) Hua, F.; Jiang, X.; Zhao, B. *Macromolecules* **2006**, *39*, 3476−3479.
(32) Yu, M.; Nowak, A. P.; Deming, T. J.; Pochan, D. J. *J. Am. Chem. Soc.* **1999**, *121*, 12210−12211.
(33) Whitmore, L.; Wallace, B. A. *Biopolymers* **2008**, *89*, 392−400.
(34) Whitmore, L.; Wallace, B. A. *Nucleic Acids Res.* **2004**, *32*, W668−W673.
(35) Mather, B. D.; Viswanathan, K.; Miller, K. M.; Long, T. E. *Prog. Polym. Sci.* **2006**, *31*, 487−531.
(36) Hoyle, C. E.; Bowman, C. N. *Angew. Chem., Int. Ed.* **2010**, *49*, 1540−1573.
(37) Tang, H. Y.; Yin, L. C.; Lu, H.; Cheng, J. J. *Biomacromolecules* **2012**, *13*, 2609−2615.
(38) Tang, H. Y.; Zhang, D. H. *Polym. Chem.* **2011**, *2*, 1542−1551.
(39) Berger, A.; Noguchi, J.; Katchalski, E. *J. Am. Chem. Soc.* **1956**, *78*, 4483−4488.
(40) Hwang, J.; Deming, T. J. *Biomacromolecules* **2001**, *2*, 17−21.
(41) Chen, C. Y.; Wang, Z. H.; Li, Z. B. *Biomacromolecules* **2011**, *12*, 2859−2863.
(42) Li, W.; Zhang, A.; Feldman, K.; Walde, P.; Schluter, A. D. *Macromolecules* **2008**, *41*, 3659−3667.
(43) Liu, Y.; Chen, P.; Li, Z. *Macromol. Rapid Commun.* **2012**, *33*, 287−295.

(44) Wang, J.; Lu, H.; Ren, Y.; Zhang, Y.; Morton, M.; Cheng, J.; Lin, Y. *Macromolecules* **2011**, *44*, 8699−8708.
(45) Haris, P. I.; Chapman, D. *Biopolymers* **1995**, *37*, 251−263.
(46) Hu, Z.; Cai, T.; Chi, C. *Soft Matter* **2010**, *6*, 2115−2123.
(47) Cheng, H.; Shen, L.; Wu, C. *Macromolecules* **2006**, *39*, 2325−2329.
(48) Cheng, Y. L.; He, C. L.; Xiao, C. S.; Ding, J. X.; Zhuang, X. L.; Chen, X. S. *Polym. Chem.* **2011**, *2*, 2627−2634.